Available online at www.sciencedirect.com
SCIENCE DIRECT®
International Journal of Mass Spectrometry 241 (2005) 225–242
International Journal of Mass Spectrometry
www.elsevier.com/locate/ijms

Influence of methylation on the properties of uracil and its noncovalent interactions with alkali metal ions Threshold collision-induced dissociation and theoretical studies

Zhibo Yang, M.T. Rodgers*

Department Of Chemistry, Wayne State University, Detroit, MI 48202, USA

Received 16 November 2004; accepted 29 November 2004
Available online 30 December 2004

Abstract

The influence of methylation on the properties of uracil and its noncovalent interactions with alkali metal ions is investigated both experimentally and theoretically. Threshold collision-induced dissociation (CID) of M^+(*x*MeU) with Xe is studied in a guided ion beam mass spectrometer. M^+ include the following alkali metal ions: Li^+, Na^+, and K^+. Five methylated uracils are examined, *x*MeU = 1-methyluracil, 3-methyluracil, 6-methyluracil, 1,3-dimethyluracil, and 5,6-dimethyluracil. In all cases endothermic loss of the intact nucleobase is the dominant reaction pathway, while ligand exchange to produce MXe^+ is observed as a minor reaction pathway. The threshold regions of the cross sections are interpreted to extract 0 and 298 K bond dissociation energies (BDEs) for M^+—*x*MeU after accounting for the effects of multiple ion-neutral collisions, kinetic and internal energies of the reactants, and dissociation lifetimes. Ab initio calculations at the MP2(full)/6–31*G** level of theory are used to determine the structures of these complexes and provide molecular constants required for the thermochemical analysis of the experimental data. Theoretical bond dissociation energies are determined from single point energy calculations at the MP2(full)/6–311+*G*(2d,2p) level using the MP2(full)/6–31*G** geometries. Excellent agreement between theory and experiment is found for the Na^+ and K^+ systems, while theory systematically underestimates the strength of binding in the Li^+ systems. Theoretical calculations are also performed to examine the influence of methylation on the acidities, proton affinities, and Watson–Crick base pairing energies. The present results are compared to earlier studies of uracil and 5-methyluracil to more fully elucidate the influence of methylation on the properties of uracil, its noncovalent interactions with alkali metal ions, and nucleic acid stability.

Keywords: Alkali metal ions; Bond dissociation energies; Collision-induced dissociation; Guided ion beams; Modified nucleobases

1. Introduction

The structure and properties of nucleic acids are profoundly influenced by their interactions with metal ions [1]. Metal ions are crucial in determining which of numerous structures nucleic acids can assume and the ways in which they pack together [2]. Metal ions represent one of the many factors that stabilize a conformer than does not require metal ions. For example, alkali metal ions are known to stabilize the B form of DNA. Binding of metal ions to the nucleobases generally leads to more profound effects on DNA conformation than binding to the phosphate backbone [3]. Metal ions have also been observed to lead to the formation and stabilization of rare or minor tautomers of the nucleobases [1]. Such modification of the nucleobases could, further, propagate into the formation of mispairs and lead to mistakes in genetic information transfer. Rare, minor, or modified nucleobases occur in small amounts in some nucleic acids. Modified nucleobases are particularly prominent in transfer RNAs, comprising up to 10% of the nucleobases present [4]. Methyl derivatives are the most common, but other functionalities are also observed, e.g., hydrogenation, thio-, or halo-substitution. Such modifications are particularly important in the study

* Corresponding author. Tel.: +1 31 35 772431; fax: +1 31 35 778822.
E-mail address: mrodgers@chem.wayne.edu (M.T. Rodgers).

1387-3806/$ – see front matter © 2004 Elsevier B.V. All rights reserved.
doi:10.1016/j.ijms.2004.11.018

of drug interactions with nucleic acids [5–8]. Nucleobase modifications, and in particular methylation, have been implicated in many forms of mutagenesis and carcinogenesis [9–12]. In addition, several methyl-substituted uracils have exhibited potent inhibitory behavior towards thymidine phosphorylase that might allow such nucleobases to be employed for anti-tumor [13], anti-cancer [14–17], anti-viral [18], and anti-HIV [19] applications. Metal complexes of derivatives of the naturally occurring nucleobases have also shown anti-tumor and anti-viral activity [20,21]. In previous work, we examined the influence of halogenation on the properties of uracil, its noncovalent interactions with alkali metal ions, and the implications for nucleic acid stability [22]. In the current study, we extend this work to examine the effects of methylation.

In this work, we use guided ion beam mass spectrometry to collisionally excite complexes of the alkali metal ions: Li^+, Na^+, and K^+, bound to a variety of methyl-substituted uracils, *x*MeU = 1-methyluracil (1-MeU), 3-methyluracil (3-MeU), 6-methyluracil (6-MeU), 1,3-dimethyluracil (1,3-diMeU), and 5,6-dimethyluracil (5,6-diMeU). The analogous complexes of the alkali metal ions with uracil (U) and thymine (T, 5-methyluracil, 5-MeU) were examined in earlier work [23,24]. The structure of uracil and the various methyl-substituted uracils examined here are shown in Fig. 1 along with their calculated dipole moments (determined here) and estimated polarizabilities [25]. The kinetic energy-dependent cross sections for the collision-induced dissociation (CID) processes are analyzed using methods developed previously [26]. The analysis explicitly includes the effects of the internal and translational energy distributions of the reactants, multiple ion-neutral collisions, and the lifetime for dissociation. M^+–*x*MeU bond dissociation energies (BDEs) are extracted for 15 complexes, and compared to theoretical BDEs calculated here. Comparison is also made to literature values for the analogous complexes of the alkali metal ions with U and 5-MeU [23,24]. The trends in the measured and calculated BDEs are examined to determine the effects of methylation on the properties of uracil and its noncovalent interactions with alkali metal ions. Theoretical calculations are also performed to examine the influence of methylation on the acidities, proton affinities, and Watson–Crick base pairing energies, and of alkali metalation on the Watson–Crick base pairing energies. The trends in these values are examined to assess the effects of methylation and alkali metalation on the stability of nucleic acids.

2. Experimental and theoretical

2.1. Experimental protocol

Cross sections for collision-induced dissociation (CID) of M^+(*x*MeU), where $M^+ = Li^+$, Na^+, and K^+, and *x*MeU = 1-MeU, 3-MeU, 6-MeU, 1,3-diMeU, and 5,6-diMeU are measured using a guided ion beam tandem mass spectrometer that has been described in detail previously [27]. The alkali metal ion-nucleobase complexes are formed by condensation of the alkali metal ion and nucleobase in a flow tube ion source operating at pressures in the range from 0.7 to 1.1 Torr. The complexes are collisionally stabilized and thermalized to room temperature by greater than 10^5 collisions with the He and Ar bath gases such that ions emanating from the source region are well described by a Maxwell–Boltzmann distribution at 298 K. The ions are extracted from the source, focused, accelerated, and focused into a magnetic sector momentum analyzer for mass analysis. Mass-selected ions are decelerated to a desired kinetic energy and focused into an octopole ion guide. The octopole passes through a static gas cell containing Xe at sufficiently low pressures that multiple ion-neutral collisions are improbable, 0.05–0.20 mTorr. The octopole ion guide acts as an efficient trap for ions in

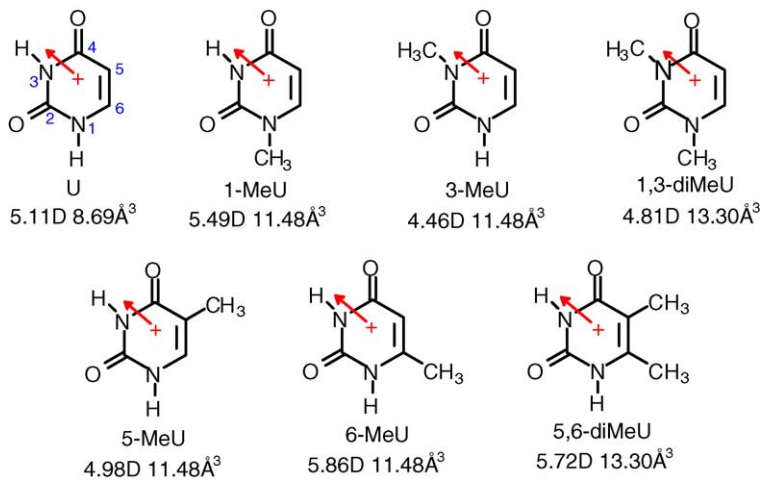

Fig. 1. Structures of uracil (U) and the methyluracils (*x*MeU). Properly scaled and oriented dipole moments in Debye are shown for each as an arrow. Dipole moments are determined from theoretical calculations performed here. The estimated polarizability is also shown [25].

the radial direction. Therefore, loss of scattered reactant and product ions in the octopole region is almost entirely eliminated [28]. Xe is used here, and in general for all of our CID measurements, because it is heavy and polarizable and therefore leads to more efficient kinetic to internal energy transfer in the CID process [29–31]. Product and unreacted beam ions drift to the end of the octopole where they are focused into a quadrupole mass filter for mass analysis and subsequently detected with a secondary electron scintillation detector and standard pulse counting techniques.

Two different quadrupole mass filters were employed in the present work, an 880 kHz and a 1.7 MHz oscillator with mass ranges that extend up to 1000 and 200 Da, respectively. The latter oscillator was purchased for use in experiments with very low mass product ions, e.g., Li^+, to overcome low mass discrimination problems encountered with the 880 kHz oscillator. The use of this new resonator significantly improved collection of low mass ions. To ensure that the use of this new oscillator did not influence our thermochemical measurements, several systems were examined using both oscillators. The shapes (energy-dependence) of the measured CID cross sections were preserved and the threshold values determined using both resonators were consistent within experimental error for all systems tested. The magnitudes of the measured CID cross sections for the systems having low mass product ions, i.e., Li^+ were found to increase, whereas the systems with heavier product ions, i.e., Na^+ and K^+ were preserved within the reported uncertainties.

2.2. Data handling

Measured ion intensities are converted to absolute cross sections using a Beer's law analysis as described previously [32]. Errors in the pressure measurement and uncertainties in the length of the interaction region result in ±20% uncertainties in the absolute cross section magnitudes, while relative uncertainties are approximately ±5%.

Ion kinetic energies in the laboratory frame, E_{lab}, are converted to energies in the center-of-mass frame, E_{CM}. All energies reported below are in the CM frame unless otherwise noted. The absolute zero and distribution of the ion kinetic energies are determined using the octopole ion guide as a retarding potential analyzer as previously described [32]. The distribution of ion kinetic energies are nearly Gaussian with a fwhm in the range from 0.2 to 0.4 (lab) for these experiments. The uncertainty in the absolute energy scale is ±0.05 eV (lab).

Because multiple ion-neutral collisions can influence the shape of CID cross sections and the threshold regions are most sensitive to these effects, each CID cross section was measured twice at three nominal pressures (0.05, 0.10, and 0.20 mTorr). Data free from pressure effects are obtained by extrapolating to zero reactant pressure, as described previously [33]. Thus, cross sections subjected to thermochemical analysis are due to single bimolecular encounters.

2.3. Theoretical calculations

Stable structures, vibrational frequencies, and energetics for the neutral, deprotonated, protonated, and alkali metalated *x*MeU nucleobases, as well as the Watson–Crick base pairs between adenine and uracil (A::U), Na^+ bound A::U base pairs, and the A::*x*MeU base pairs, were obtained from ab initio electronic structure calculations using Gaussian 98 [34]. Geometry optimizations and vibrational analyses were performed at the MP2(full)/6–31*G** level for all systems except the base pairs where the larger size of these systems required the use of the B3LYP/6–31*G** level of theory. When used to model the data or to calculate thermal energy corrections, the MP2(full)/6–31*G** and B3LYP/6-31*G** vibrational frequencies are scaled by factors of 0.9646 and 0.9804, respectively. The vibrational frequencies and rotational constants of the M^+(*x*MeU) complexes and *x*MeU neutral nucleobases are listed in Tables 1 and 2. Single point energy calculations were performed at the MP2(full)/6–311+*G*(2d,2p) level using the MP2(full)/6–31*G** and B3LYP/6–31*G** geometries. Zero point energy (ZPE) and basis set superposition error (BSSE) corrections were included in the determination of the BDEs. In very limited cases, the complete basis set extrapolation protocol (CBS-Q) was also employed to help further assess the accuracy of the theoretical calculations.

2.4. Thermochemical analysis

The threshold regions of the reaction cross sections are modeled using Eq. (1)

$$\sigma(E) = \frac{\sigma_0 \sum_i g_i (E + E_i - E_0)^n}{E} \quad (1)$$

where σ_0 is an energy independent scaling factor; E, the relative translational energy of the reactants; E_0, the threshold for reaction of the ground electronic and ro-vibrational state; and n is an adjustable parameter that describes the efficiency of kinetic to internal energy transfer [35]. The summation is over the ro-vibrational states of the reactant ions, i, where E_i is the excitation energy of each ro-vibrational state and g_i, the population of those states ($\Sigma g_i = 1$). The populations of excited ro-vibrational levels are not negligible even at 298 K as a result of the many low-frequency modes present in these ions. The relative reactivity of all ro-vibrational states, as reflected by σ_0 and n, is assumed to be equivalent.

The Beyer-Swinehart algorithm [36] is used to evaluate the density of the ro-vibrational states, and the relative populations, g_i, are calculated for a Maxwell–Boltzmann distribution at the 298 K temperature appropriate for the reactants. The vibrational frequencies of the reactant complexes are determined from ab initio theory calculations as discussed in the Theoretical Calculations section. The average vibrational energy at 298 K of the M^+(*x*MeU) complexes is given in Table 1. To account for the inaccuracies in the computed frequencies, we have increased and decreased the prescaled frequencies

Table 1
Vibrational frequencies and average vibrational energies at 298 K[a]

Species	E_{vib} (eV)[b]	Frequencies (cm^{-1})
1-MeU	0.18 (0.02)	61, 104, 152, 215, 324, 373, 377, 453, 525, 608, 661, 692, 704, 745, 764, 781, 891, 959, 1035, 1141, 1155, 1197, 1229, 1335, 1368, 1393, 1452, 1466, 1479, 1519, 1651, 1761, 1772, 3020, 3109, 3127, 3141, 3186, 3483
Li^+(1-MeU)	0.22 (0.02)	74, 83, 100, 128, 171, 266, 320, 369, 399, 413, 517, 610, 628, 673, 691, 723, 752, 755, 824, 922, 995, 1051, 1139, 1148, 1182, 1224, 1343, 1368, 1394, 1460, 1475, 1498, 1527, 1632, 1683, 1799, 3032, 3131, 3145, 3153, 3192, 3457
Na^+(1-MeU)	0.24 (0.02)	47, 49, 94, 123, 165, 244, 257, 320, 372, 395, 477, 546, 610, 671, 692, 716, 752 (2), 796, 917, 985, 1048, 1139, 1152, 1183, 1229, 1343, 1364, 1393, 1459, 1476, 1493, 1521, 1637, 1698, 1794, 3031, 3128, 3142, 3151, 3190, 3466
K^+(1-MeU)	0.24 (0.02)	40, 43, 89, 123, 161, 170, 250, 321, 374, 393, 469, 540, 611, 671, 693, 711, 751, 753, 791, 913, 979, 1046, 1140, 1155, 1184, 1232, 1343, 1363, 1393, 1459, 1477, 1488, 1519, 1641, 1711, 1790, 3030, 3126, 3140, 3150, 3188, 3473
3-MeU	0.18 (0.02)	79, 126, 151, 210, 342, 386, 390, 490, 527, 556, 571, 676, 695, 705, 762, 845, 887, 978, 1071, 1126, 1146, 1159, 1225, 1286, 1383, 1406, 1440, 1490, 1498, 1509, 1654, 1731, 1775, 3030, 3113, 3150, 3158, 3188, 3525
Li^+(3-MeU)	0.22 (0.02)	71, 89, 117, 140, 180, 239, 344, 392, 420, 444, 523, 568, 630, 646, 685, 712, 729, 751, 859, 918, 998, 1090, 1123, 1141, 1163, 1234, 1274, 1383, 1418, 1454, 1499 (2), 1534, 1612, 1671, 1803, 3032, 3123, 3162, 3163, 3192, 3478
Na^+(3-MeU)	0.23 (0.02)	47, 51, 108, 140, 173, 232, 244, 352, 393, 414, 513, 547, 571, 633, 683, 709 (2), 748, 850, 913, 990, 1087, 1125, 1142, 1163, 1233, 1280, 1382, 1415, 1449, 1500, 1502, 1524, 1625, 1681, 1798, 3029, 3118, 3160, 3161, 3190, 3486
K^+(3-MeU)	0.23 (0.02)	40, 41, 107, 141, 170 (2), 228, 350, 395, 410, 508, 539, 572, 623, 685, 707, 709, 751, 849, 909, 987, 1085, 1126, 1143, 1163, 1232, 1283, 1381, 1413, 1446, 1501, 1504, 1517, 1634, 1690, 1795, 3026, 3112, 3159 (2), 3189, 3493
6-MeU	0.18 (0.02)	124, 126, 153, 195, 289, 368, 466, 485, 510, 554, 561, 619, 667, 696, 709, 778, 933, 964, 1020, 1048, 1052, 1177, 1231, 1326, 1365, 1403, 1419, 1479, 1485, 1508, 1671, 1761, 1799, 2996, 3071, 3111, 3177, 3489, 3510
Li^+(6-MeU)	0.23 (0.02)	81, 82, 107, 149, 190, 197, 292, 363, 451, 500, 523, 558, 577, 638, 671, 704, 719, 720, 761, 942, 997, 1029, 1049, 1059, 1192, 1218, 1330, 1365, 1420, 1441, 1480, 1482, 1543, 1626, 1682, 1826, 3003, 3081, 3120, 3185, 3464, 3467
Na^+(6-MeU)	0.24 (0.02)	48, 52, 113, 146, 186, 191, 243, 298, 368, 497, 516, 535, 561, 623, 646, 669, 701, 715, 759, 942, 987, 1027, 1049, 1055, 1188, 1227, 1328, 1365, 1420, 1432, 1481, 1482, 1532, 1638, 1698, 1821, 3002, 3080, 3118, 3183, 3473, 3475
K^+(6-MeU)	0.24 (0.02)	42, 44, 117, 143, 170, 181, 192, 295, 370, 495, 510, 527, 563, 612, 637, 667, 703, 712, 760, 942, 982, 1026, 1050, 1053, 1186, 1231, 1328, 1365, 1420, 1425, 1481, 1482, 1526, 1646, 1710, 1818, 3002, 3079, 3117, 3181, 3479, 3481
1,3-diMeU	0.23 (0.02)	67, 91, 109, 128, 195, 238, 314, 358, 396, 399, 470, 501, 610, 670, 674, 699, 757, 787, 884, 936, 1009, 1079, 1139, 1140, 1145, 1166, 1244, 1286, 1352, 1389, 1429, 1460, 1472, 1478, 1498, 1508, 1520, 1652, 1727, 1748, 3020, 3030, 3110, 3113, 3126, 3141, 3160, 3184
Li^+(1,3-diMeU)	0.27 (0.02)	66, 88, 97, 121, 126, 156, 223, 278, 313, 355, 397, 425, 427, 499, 606, 634, 678, 691, 696, 747, 823, 913, 938, 1023, 1067, 1137, 1142, 1148, 1175, 1225, 1271, 1358, 1394, 1430, 1461, 1475, 1498, 1500 (2), 1529, 1615, 1671, 1770, 3032 (2), 3123, 3131, 3144, 3153, 3164, 3189
Na^+(1,3-diMeU)	0.28 (0.02)	42, 50, 95, 115, 121, 151, 218, 242, 270, 315, 361, 401, 420, 488, 521, 614, 678, 687, 696, 744, 798, 908, 939, 1017, 1071, 1138, 1143, 1147, 1173, 1230, 1277, 1356, 1391, 1429, 1461, 1475, 1497, 1500, 1501, 1524, 1626, 1680, 1765, 3029, 3030, 3117, 3128, 3142, 3152, 3162, 3187
K^+(1,3-diMeU)	0.28 (0.02)	35, 39, 94, 114, 117, 149, 170, 213, 264, 314, 361, 401, 416, 483, 513, 615, 681, 685, 697, 746, 795, 905, 939, 1015, 1072, 1138, 1143, 1146, 1173, 1233, 1280, 1355, 1389, 1429, 1461, 1476, 1493, 1501, 1504, 1521, 1634, 1689, 1762, 3026, 3030, 3112, 3127, 3140, 3150, 3160, 3185
5,6-diMeU	0.24 (0.02)	46, 69, 101, 129, 169, 291, 301, 315, 378, 449, 461, 504, 556, 606, 609, 664, 696, 717, 756, 938, 960, 1039, 1045, 1056, 1122, 1184, 1232, 1302, 1366, 1408, 1413, 1418, 1486, 1488, 1489, 1514 (2), 1671, 1735, 1799, 2994, 2997, 3064, 3071, 3109, 3125, 3488, 3508
Li^+(5,6-diMeU)	0.28 (0.02)	38, 78, 80, 100, 116, 166, 198, 286, 299, 314, 365, 435, 489, 515, 554, 605, 644, 667, 706, 720, 721, 761, 953, 977, 1030, 1036, 1048, 1137, 1221, 1227, 1285, 1365, 1418, 1424, 1446, 1472, 1486, 1493, 1504, 1550, 1625, 1656, 1824, 3001, 3008, 3072, 3094, 3103, 3120, 3464, 3473
Na^+(5,6-diMeU)	0.29 (0.02)	18, 46, 51, 93, 112, 161, 190, 239, 284, 304, 318, 372, 461, 508, 524, 606, 629, 641, 666, 703, 718, 760, 948, 974, 1030, 1036, 1048, 1133, 1215, 1235, 1286, 1365, 1417, 1423, 1439, 1474, 1487, 1493, 1504, 1539, 1638, 1670, 1820, 2999, 3008, 3069, 3094, 3102, 3118, 3472, 3482
K^+(5,6-diMeU)	0.30 (0.02)	34, 36, 42, 80, 108, 156, 168, 183, 285, 312, 334, 376, 457, 502, 521, 607, 616, 629, 667, 705, 719, 759, 942, 968, 1035, 1042, 1053, 1129, 1210, 1236, 1291, 1366, 1414, 1424, 1432, 1477, 1485, 1495, 1510, 1528, 1648, 1684, 1817, 2999, 3006, 3068, 3085, 3113, 3124, 3478, 3485

[a] Vibrational frequencies (scaled by 0.9646) are obtained from a vibrational analysis of the geometry optimized structures for these species obtained from ab initio calculations performed at the MP2(full)/6–31*G** level, degeneracies are listed in parentheses.

[b] Uncertainties listed in parentheses are determined as described in the text.

Table 2
Rotational constants of M^+(*x*MeU) in cm^{-1}

Reactant	Energized molecule		Transition state		
	D[a]	2D[b]	ID[a]	2D[c]	2D[b,d]
Li^+(1-MeU)	0.11	0.030	0.11	0.040	0.068
Na^+(1-MeU)	0.11	0.019	0.11	0.040	0.0095
K^+(1-MeU)	0.11	0.013	0.11	0.040	0.0047
Li^+(3-MeU)	0.078	0.037	0.079	0.049	0.053
Na^+(3-MeU)	0.078	0.023	0.079	0.049	0.0076
K^+(3-MeU)	0.078	0.016	0.079	0.049	0.0028
Li^+(6-MeU)	0.065	0.033	0.067	0.044	0.059
Na^+(6-MeU)	0.065	0.020	0.067	0.044	0.0082
K^+(6-MeU)	0.065	0.014	0.067	0.044	0.0043
Li^+(1,3-diMeU)	0.074	0.027	0.075	0.035	0.057
Na^+(1,3-diMeU)	0.074	0.018	0.075	0.035	0.0076
K^+(1,3-diMeU)	0.074	0.013	0.075	0.035	0.0027
Li^+(5,6-diMeU)	0.049	0.029	0.060	0.034	0.068
Na^+(5,6-diMeU)	0.048	0.019	0.060	0.034	0.0065
K^+(5,6-diMeU)	0.048	0.014	0.060	0.034	0.0034

[a] Active external.
[b] Inactive external.
[c] Rotational constants of the transition state treated as free internal rotors.
[d] Two-dimensional rotational constant of the transition state at the threshold energy for dissociation, treated variationally and statistically.

by 10%. This encompasses the range of scale factors needed to bring calculated frequencies into agreement with experimentally determined frequencies found by Pople et al. [37] The corresponding change in the average vibrational energy is taken to be an estimate of one standard deviation of the uncertainty in the vibrational energy (Table 1).

Statistical theories for unimolecular dissociation (Rice-Ramsperger-Kassel-Marcus (RRKM) theory) of the collisionally activated ions are also included in Eq. (1) to account for the possibility that these ions may not have undergone dissociation prior to arriving at the detector ($\sim 10^{-4}$ s) [26,38]. In our analysis, we assume that the transition states (TSs) are loose and product-like because the interaction between the alkali metal ion and the nucleobase is largely electrostatic. The best model for the TS of such electrostatically bound complexes is a loose phase space limit (PSL) model located at the centrifugal barrier for the interaction of M^+ with *x*MeU as described in detail elsewhere [26]. The parameters appropriate for the PSL model TS are the frequencies and rotational constants of the products. Ro-vibrational frequencies appropriate for the energized molecules and the transition states leading to dissociation are given in Tables 1 and 2.

The model represented by Eq. (1) is expected to be appropriate for translationally driven reactions [39] and has been found to reproduce CID cross sections well. The model is convoluted with the kinetic energy distributions of both the reactant M^+(*x*MeU) complex and neutral Xe atom, and a nonlinear least-squares analysis of the data is performed to give optimized values for the parameters σ_0, E_0, and n. The error associated with the measurement of E_0 is estimated from the range of threshold values determined for the eight zero-pressure-extrapolated data sets, variations associated with uncertainties in the vibrational frequencies (scaling as discussed above), and the error in the absolute energy scale, 0.05 eV (lab). For analyses that include the RRKM lifetime analysis, the uncertainties in the reported E_0(PSL) values also include the effects of increasing and decreasing the time assumed available for dissociation by a factor of 2.

Eq. (1) explicitly includes the internal energy of the ion, E_i. All energy available is treated statistically because the internal energy of the reactants is redistributed throughout the ion upon collision with Xe. Because the CID processes examined here are simple noncovalent bond fission reactions, the E_0(PSL) values determined by analysis with Eq. (1) can be equated to 0 K BDEs [40,41].

3. Results

3.1. Cross sections for collision-induced dissociation

Experimental cross sections were obtained for the interaction of Xe with 15 M^+(*x*MeU) complexes, where $M^+ = Li^+$, Na^+, and K^+, and *x*MeU = 1-MeU, 3-MeU, 6-MeU, 1,3-diMeU, and 5,6-diMeU. Fig. 2 shows representative data for the M^+(1-MeU) complexes. Analogous behavior is observed for all other M^+(*x*MeU) complexes. As shown in Fig. 2 for the M^+(1-MeU) complexes, the dominant process for all complexes is the loss of the intact nucleobase base in the CID reaction (2):

$$M^+(x\text{MeU}) + \text{Xe} \rightarrow M^+ + x\text{MeU} + \text{Xe} \quad (2)$$

The magnitudes of the cross sections increase with increasing size of the alkali metal ion, primarily because the strength of the noncovalent interaction between the alkali metal ion and the nucleobase decreases in this same order. Ligand exchange processes to form MXe^+ are also observed as very minor reaction pathways in several of the systems examined here, reaction (3):

$$M^+(x\text{MeU}) + \text{Xe} \rightarrow MXe^+ + x\text{MeU} \quad (3)$$

However, the cross sections for ligand exchange are more than two orders of magnitude smaller than those for the primary CID pathway. It is likely that this ligand exchange process occurs for all complexes, but that the signal to noise in the other experiments was not sufficient to differentiate the M^+Xe product from background noise. Because little systematic information can be extracted from these ligand exchange products, they will not be discussed further.

3.2. Threshold analysis

The model of Eq. (1) was used to analyze the thresholds for reactions (2) in 15 M^+(*x*MeU) systems. The results of these analyses are provided in Table 3. Representative results are shown in Fig. 3 for the M^+(1-MeU) complexes. Analogous behavior is observed for all other M^+(*x*MeU) complexes. In every case, the experimental cross sections for re-

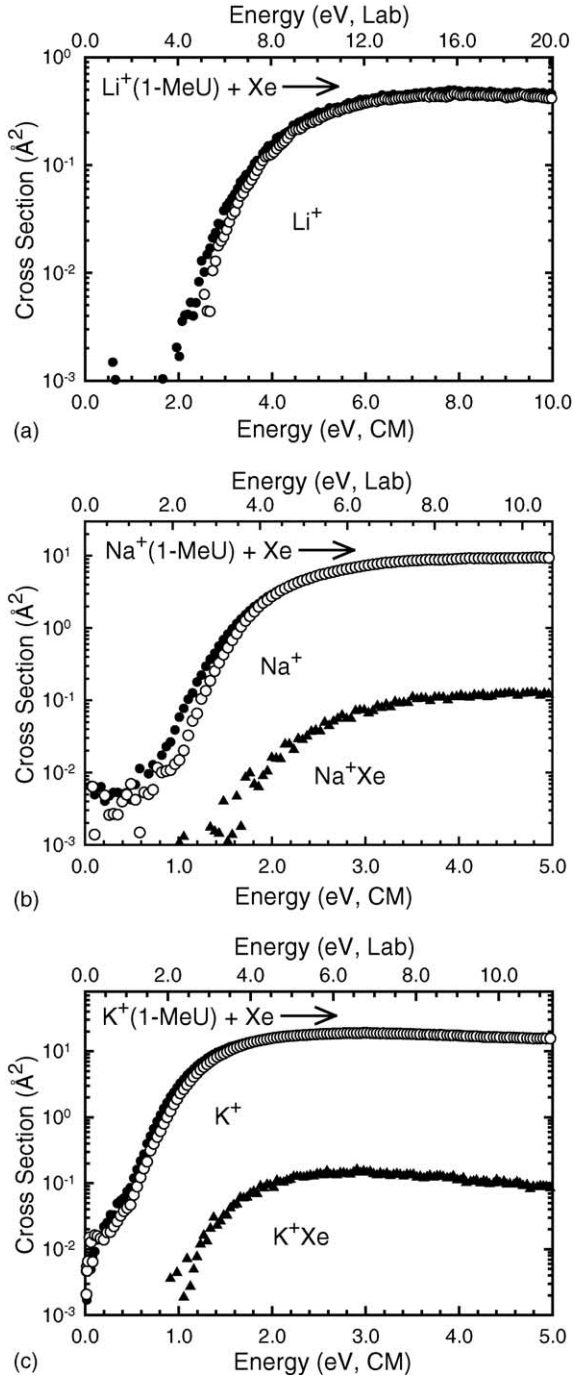

Fig. 2. Cross sections for the collision-induced dissociation of the M^+(1-MeU) complexes with Xe as a function of collision energy in the center-of-mass frame (lower *x*-axis) and laboratory frame (upper *x*-axis), where $M^+ = Li^+$, Na^+, K^+, parts a-c, respectively. Data for M^+ product channel are shown for a Xe pressure of 0.2 mTorr (●) and extrapolated to zero (○). The cross section for the ligand exchange process to form M^+Xe is also shown when observed (▲).

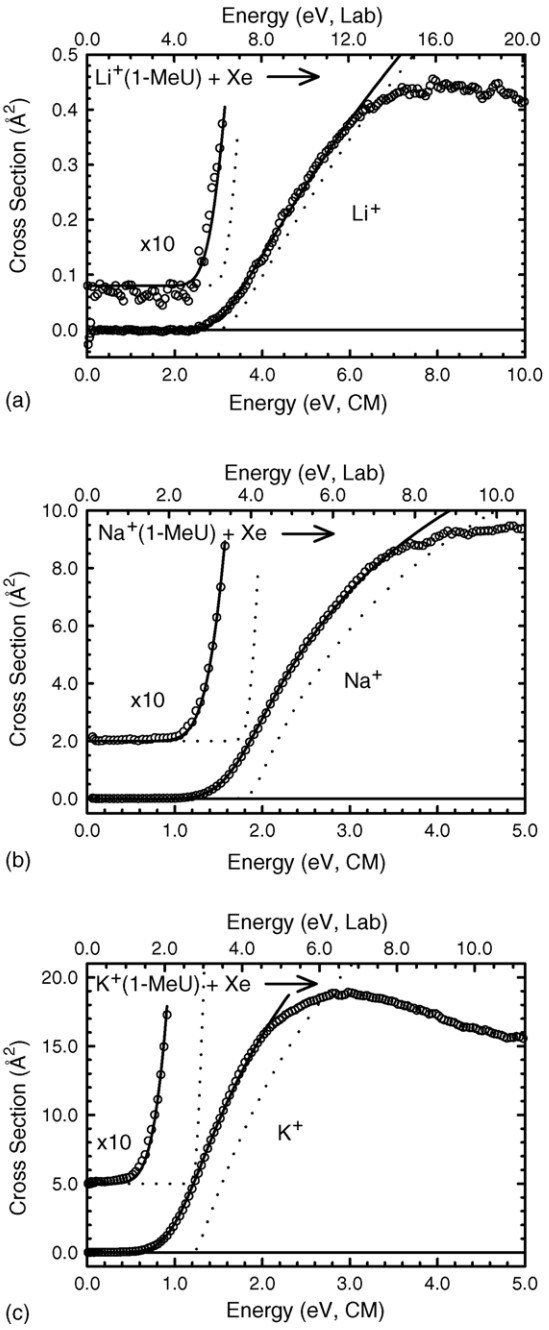

Fig. 3. Zero pressure extrapolated cross section for collision-induced dissociation of M^+(1-MeU) complexes with Xe in the threshold region as a function of kinetic energy in the center-of-mass frame (lower *x*-axis) and laboratory frame (upper *x*-axis), where $M^+ = Li^+$, Na^+, K^+, parts a-c, respectively. The solid line shows the best fit to the data using Eq. (1) convoluted over the neutral and ion kinetic and internal energy distributions. The dotted line shows the model cross sections in the absence of experimental kinetic energy broadening for reactants with an internal energy corresponding to 0 K.

actions (2) are accurately reproduced using a loose PSL TS model.[26] Previous work has shown that this model provides the most accurate assessment of the kinetic shifts for CID processes for noncovalently bound ion-molecule complexes [22,23,26,27,42–57] Good reproduction of the data is obtained over energy ranges exceeding 2 eV and cross section magnitudes of at least a factor of 100. Table 3 also includes threshold values obtained without including the RRKM lifetime analysis. The difference between these values and those obtained including the lifetime analysis shows that the kinetic

Table 3
Threshold dissociation energies at 0 k and entropies of activation at 1000 K of M^+L[a]

M^+L	σ_0[b]	n[b]	E_0[c] (eV)	E_0(PSL) (eV)	Kinetic shift[d] (eV)	$\Delta S^\dagger$(PSL) (J mol^{-1} K^{-1})
Li^+(1-MeU)	0.5 (0.1)	1.4 (0.1)	3.12 (0.05)	2.43 (0.07)	0.69	29 (2)
Na^+(1-MeU)	15.0 (0.5)	1.1 (0.1)	1.83 (0.03)	1.56 (0.04)	0.27	26 (2)
K^+(1-MeU)	32.8 (1.0)	1.2 (0.1)	1.24 (0.03)	1.15 (0.03)	0.09	22 (2)
Li^+(3-MeU)	0.4 (0.1)	1.5 (0.1)	2.89 (0.06)	2.29 (0.07)	0.60	31 (2)
Na^+(3-MeU)	14.7 (0.3)	1.2 (0.1)	1.71 (0.03)	1.49 (0.04)	0.22	28 (2)
K^+(3-MeU)	28.6 (1.2)	1.2 (0.1)	1.17(0.05)	1.11 (0.03)	0.06	36 (2)
Li^+(6-MeU)	0.2 (0.1)	1.6 (0.1)	2.97 (0.04)	2.30 (0.07)	0.67	26 (2)
Na^+(6-MeU)	15.4 (1.7)	1.5 (0.1)	1.62 (0.08)	1.42 (0.06)	0.20	24 (2)
K^+(6-MeU)	32.3 (2.5)	1.1 (0.1)	1.22 (0.08)	1.13 (0.06)	0.09	20 (2)
Li^+(1,3-diMeU)	0.5 (0.1)	1.4 (0.1)	3.48 (0.06)	2.49 (0.08)	0.99	32 (2)
Na^+(1,3-diMeU)	15.8 (0.6)	1.2 (0.1)	2.00 (0.04)	1.59(0.05)	0.41	29 (2)
K^+(1,3-diMeU)	23.4 (1.6)	1.2 (0.1)	1.40 (0.04)	1.23 (0.03)	0.17	38 (2)
Li^+(5,6-diMeU)	0.5 (0.1)	1.2 (0.1)	3.45 (0.07)	2.42 (0.07)	1.03	29 (2)
Na^+(5,6-diMeU)	10.5 (1.2)	1.5 (0.1)	1.79 (0.06)	1.42 (0.05)	0.37	22 (2)
K^+(5,6-diMeU)	40.8 (0.9)	0.9 (0.1)	1.38 (0.03)	1.17 (0.03)	0.21	21 (2)

[a] Uncertainties are listed in parentheses.
[b] Average values for loose PSL transition state.
[c] No RRKM analysis.
[d] Difference between E_0 and E_0(PSL).

shifts observed for these systems are largest for the complexes to Li^+ (0.60–1.03 eV), decrease for the complexes to Na^+ (0.20–0.41 eV), and are the smallest for the complexes to K^+ (0.06–0.21 eV). The observed kinetic shifts should correlate directly with the density of states of the complex at threshold, which depends on the measure BDE, as observed (Table 3). The total number of vibrational modes varies for these M^+(*x*MeU) complexes: 42 for methyluracils (1-MeU, 3-MeU, and 6-MeU), and 51 for the dimethyluracils (1,3-dimeu and 5,6-diMeU). The increased number of modes available in the complexes to the dimethyluracils leads to a greater density of states and, thus, larger kinetic shifts than observed for the complexes to the methyluracils.

The entropy of activation, $\Delta S^\dagger$, is a measure of the looseness of the TS and also a reflection of the complexity of the system. It is largely determined by the molecular parameters used to model the energized molecule and the TS, but also depends on the threshold energy. Listed in Table 3, $\Delta S^\dagger$(PSL) values at 1000 K show modest variations, as expected based on the similarity of these systems. The $\Delta S^\dagger$(PSL) values typically decrease with increasing size of the alkali metal ion, and vary between 21 and 38 J K^{-1} mol^{-1} across these systems. These entropies of activation compare favorably to a wide variety of noncovalently bound complexes previously measured in our laboratory [22,23,26,27,42–57].

3.3. Theoretical results

Theoretical structures for the neutral, deprotonated, protonated, and alkali metalated *x*MeU nucleobases, as well as the A::U, Na^+ bound A::U, and A::*x*MeU Watson–Crick base pairs between the *x*MeU nucleobases and adenine, were calculated as described above. Structures of the most stable conformations of the Na^+–*x*MeU complexes are shown in Fig. 4 for each base. Structures for the complexes to the other alkali metal ions are very similar except for the M^+–*x*MeU bond distance. The 0 K calculated proton and metal ion binding energies, performed at the MP2(full)/6–311+*G*(2d,2p)//MP2(full)/6–31*G** level are listed in Table 4 . Independent ZPE and BSSE corrections are made for all complexes. Values for H^+, Li^+, and Na^+ binding to U determined at the CBS-Q level are also given in Table 4. Geometrical parameters of the ground state MP2(full)/6–31*G** geometry optimized structures of the neutral, protonated, and alkali metalated *x*MeU nucleobases are summarized in Table 5. The 0 K calculated acidities of the *x*MeU nucleobases are listed in Table 6. The 0 K calculated base pairing energies of the A::*x*MeU and the Na^+(A::*x*MeU) Watson–Crick base pair complexes are listed in Table 7, while the optimized structures of these species are shown in Figs. 5 and 6, respectively.

3.4. Dipole moments

The calculated dipole moments of uracil and its methylated analogs are summarized in Fig. 1. As shown in the figure, the dipole moment of uracil is relatively large, 5.11 D, and is oriented nearly parallel to the N3-C6 direction but slightly offset toward C4. As can be seen in the figure, the magnitudes of the dipole moments of the *x*MeU nucleobases are sensitive to the position(s) of methylation, whereas their orientations are relatively unaffected. Methyl substitution at the 3- or 5- positions leads to a decrease in the dipole moment of 0.65 and 0.13 D, whereas substitution at the 1- or 6- positions leads to an increase in the dipole moment of 0.38 and 0.75 D, respectively. As expected, the effects are the great-

Table 4
Calculated enthalpies of proton and alkali metal ion binding to methylated uracils at 0 K in kJ/mol

Complex	Experiment			Binding site	Theory			
	TCID[a]	Literature			MP2(full)			CBS-Q
			Adjusted		D_e[b]	D_0[b,c]	$D_{0,BSSE}$[b,d]	D_0
H^+(U)		866.6[e]		O4	879.5	846.7	837.5	851.2
		868 (13)[f]		O4	867.6	835.5	826.4	
		835 (13)[f]		O2	845.2	815.1	805.8	
				O2	840.2	810.4	801.0	
Li^+(U)	211.5 (6.1)[g]	209.4 (4)[h]	197 (20)[h]	O4	207.5	201.2	194.9	200.9
				O2	192.0	186.7	180.5	
				π	68.3	65.0	56.5	
Na^+(U)	134.6 (3.4)[g]	140 (4)[h]	129 (25)[h]	O4	146.2	142.5	134.5	142.9
				O2	132.6	129.7	122.8	
K^+(U)	104.3 (2.8)[g]	100 (4)[h]	96 (12)[h]	O4	110.8	107.8	103.8	
				O2	98.4	96.1	92.2	
H^+(1-MeU)				O4	899.5	867.1	857.8	
				O4	887.6	855.8	846.1	
				O2	859.8	829.6	820.3	
				O2	855.4	825.3	815.8	
Li^+(1-MeU)	234.0 (7.2)			O4	219.1	212.9	206.6	
				O2	195.5	190.1	183.9	
Na^+(1-MeU)	150.7 (4.1)			O4	155.5	151.9	144.9	
				O2	134.4	131.5	124.4	
K^+(1-MeU)	110.9 (2.7)			O4	118.8	115.9	111.9	
				O2	99.5	97.2	93.2	
H^+(3-MeU)				O4	899.0	866.2	856.8	
				O4	889.2	856.6	847.1	
				O2	867.2	836.6	827.1	
				O2	858.8	829.4	820.0	
Li^+(3-MeU)	220.9 (6.7)			O4	214.0	207.7	201.4	
				O2	198.3	193.0	186.7	
Na^+(3-MeU)	143.6 (3.8)			O4	150.4	146.6	139.5	
				O2	136.6	133.7	126.6	
K^+(3-MeU)	107.5 (3.3)			O4	114.0	111.0	106.8	
				O2	99.5	97.8	93.7	
H^+(5-MeU)[f]		874.8[e]		O4	886.8	854.4	844.9	
				O4	875.5	843.6	834.5	
				O2	860.0	830.2	820.9	
				O2	855.5	825.9	816.6	
Li^+(5-MeU)	210.1 (7.0)[g]	213 (4)[h]	200 (20)[h]	O4	208.3	202.2	195.8	
				O2	201.0	195.8	189.6	
				π	79.0	75.6	66.6	
Na^+(5-MeU)	135.3 (3.8)[g]	143 (4)[h]	136 (25)[h]	O4	146.0	142.4	135.2	
				O2	140.0	137.2	130.2	
K^+(5-MeU)	104.0 (3.8)[g]	101 (4)[h]	97 (12)[h]	O4	110.4	107.6	103.4	
				O2	104.7	102.6	98.6	
H^+(6-MeU)				O4	897.2	865.3	856.0	
				O4	885.4	854.1	845.0	
				O2	858.8	828.9	819.6	
				O2	853.3	823.7	814.4	
Li^+(6-MeU)	222.3 (6.6)			O4	217.1	211.2	204.8	
				O2	199.4	194.3	188.0	
Na^+(6-MeU)	136.6 (5.8)			O4	153.8	150.4	143.3	
				O2	138.7	136.0	128.9	
K^+(6-MeU)	108.8 (5.4)			O4	117.3	114.5	110.5	
				O2	103.6	101.5	97.4	
H^+(1,3-diMeU)				O4	918.2	885.6	876.3	
				O4	907.7	875.4	865.9	
				O2	880.7	849.9	840.3	
				O2	872.3	842.5	832.9	
Li^+(1,3-diMeU)	239.8 (7.8)			O4	225.1	218.9	212.6	
				O2	201.5	196.1	189.7	
Na^+(1,3-diMeU)	153.6 (4.7)			O4	159.3	155.7	148.5	
				O2	138.3	135.3	127.9	

Table 4 (*Continued*)

Complex	Experiment		Binding site	Theory			
	TCID[a]	Literature		MP2(full)			CBS-Q
		Adjusted		D_e[b]	D_0[b,c]	$D_{0,BSSE}$[b,d]	D_0
K^+(1,3-diMeU)	118.9 (3.3)		O4	121.8	118.9	114.7	
			O2	102.8	100.4	96.1	
H^+(5,6-diMeU)			O4	906.4	873.4	864.4	
			O4	895.0	863.4	854.1	
			O2	873.0	843.3	834.0	
			O2	868.2	838.8	829.5	
Li^+(5,6-diMeU)	233.8 (6.5)		O4	218.5	212.4	206.0	
			O2	207.8	202.8	196.5	
Na^+(5,6-diMeU)	136.8 (5.1)		O4	153.9	150.5	143.2	
			O2	145.6	143.0	135.9	
K^+(5,6-diMeU)	113.2 (3.2)		O4	117.3	113.9	109.6	
			O2	109.5	107.6	103.5	

[a] Threshold collision-induced dissociation. Present results except as noted.
[b] Calculated at the MP2(full)/6–311+*G*(2d,2p) level of theory using MP2(full)/6–31*G** ground state optimized geometries.
[c] Including zero-point energy corrections with frequencies scaled by 0.9646.
[d] Also includes basis set superposition error corrections.
[e] Hunter and Lias, Proton affinity evaluation NIST Chemistry WebBook, adjusted to 0 K [60].
[f] Kurinovich et al., adjusted to 0 K [61].
[g] Rodgers and Armentrout [23].
[h] Cerda and Wesdemiotis (adjusted to 0 K as described in [23]) [24].

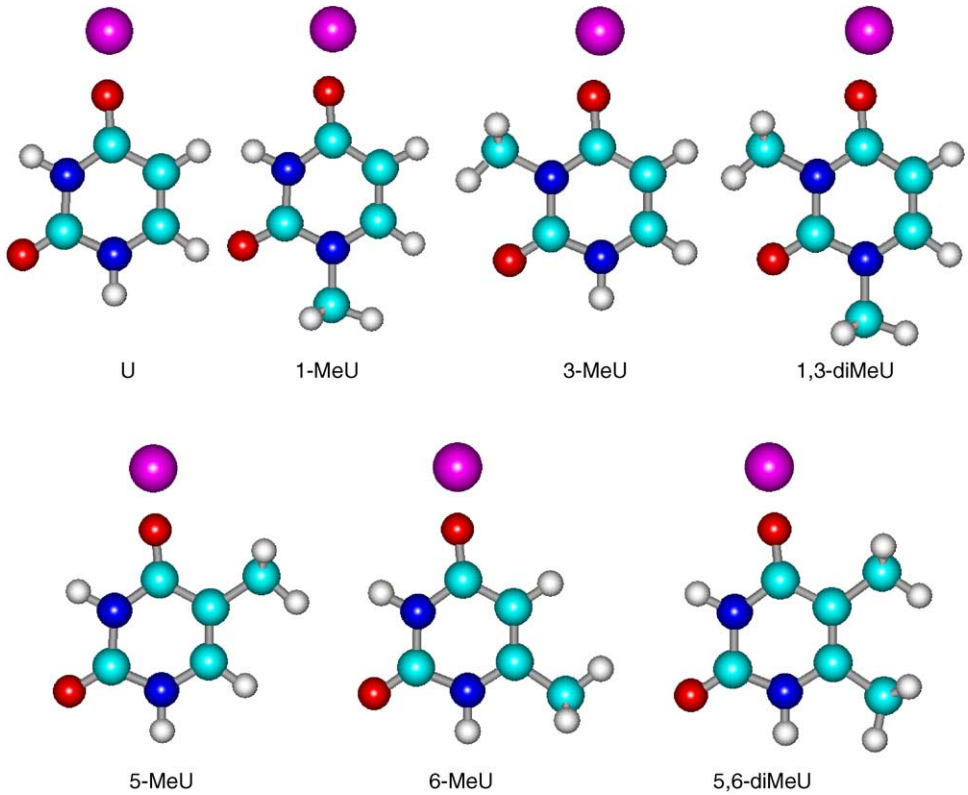

Fig. 4. MP2(full)/6–31*G** optimized geometries of Na^+(*x*MeU), where *x*MeU = U, 1-MeU, 3-MeU, 1,3-diMeU, 5-MeU, 6-MeU, and 5,6-diMeU.

Table 5
Geometrical parameters of MP2(full)/6–31*G** geometry optimized structures of neutral, protonated, and alkali metalated methyluracils

Species	O4 Binding				O2 binding			
	Bond distance (Å)			Bond angle (°)	Bond distance (Å)			Bond angle (°)
	C═O	M^+─O	N3─H	∠COM$^+$	C═O	M^+─O	N3─H	∠COM$^+$
U[a]	1.226	–	1.017	–	1.223	–	1.017	–
H^+(U)[a]	1.315	0.980	1.024	112.4	1.315	0.979	1.025	114.8
Li^+(U)[a]	1.263	1.750	1.019	171.9	1.262	1.755	1.018	173.4
Na^+(U)[a]	1.255	2.109	1.019	173.2	1.253	2.116	1.018	173.0
K^+(U)[a]	1.249	2.482	1.018	174.7	1.247	2.493	1.018	173.1
1-MeU	1.228	–	1.017	–	1.226	–	1.017	–
H^+(1-MeU)	1.319	0.979	1.023	112.0	1.321	0.979	1.022	113.5
Li^+(1-MeU)	1.265	1.744	1.020	171.4	1.266	1.751	1.019	170.9
Na^+(1-MeU)	1.257	2.102	1.109	172.6	1.257	2.113	1.018	170.9
K^+(1-MeU)	1.251	2.473	1.018	174.3	1.251	2.488	1.017	171.6
3-MeU	1.230	–	–	–	1.226	–	–	–
H^+(3-MeU)	1.321	0.979	–	111.5	1.319	0.979	-	113.2
Li^+(3-MeU)	1.267	1.746	–	169.2	1.266	1.749	-	174.6
Na^+(3-MeU)	1.259	2.104	–	170.9	1.257	2.110	-	173.9
K^+(3-MeU)	1.252	2.477	–	173.6	1.251	2.486	-	176.8
5-MeU[a]	1.229	–	1.017	–	1.224	–	1.017	–
H^+(5-MeU)[a]	1.317	0.980	1.024	111.9	1.318	0.979	1.022	114.0
Li^+(5-MeU)[a]	1.266	1.747	1.019	174.7	1.264	1.750	1.019	173.9
Na^+(5-MeU)[a]	1.257	2.107	1.019	175.9	1.255	2.110	1.018	173.5
K^+(5-MeU)[a]	1.249	2.500	1.018	180.0	1.249	2.485	1.017	173.6
6-MeU	1.227	-	1.017	–	1.224	–	1.017	–
H^+(6-MeU)	1.318	0.979	1.023	112.1	1.317	0.979	1.022	113.9
Li^+(6-MeU)	1.265	1.743	1.020	172.4	1.263	1.753	1.018	172.6
Na^+(6-MeU)	1.256	2.102	1.018	173.7	1.254	2.112	1.017	172.5
K^+(6-MeU)	1.251	2.474	1.017	175.2	1.249	2.486	1.017	172.5
1,3-diMeU	1.231	–	–	–	1.230	–	–	–
H^+(1,3-diMeU)	1.324	0.979	–	111.4	1.323	0.979	–	112.7
Li^+(1,3-diMeU)	1.270	1.739	–	168.7	1.268	1.747	–	170.9
Na^+(1,3-diMeU)	1.261	2.098	–	170.3	1.259	2.108	–	170.8
K^+(1,3-diMeU)	1.254	2.467	–	173.2	1.253	2.482	–	169.5
5,6-diMeU	1.231	–	1.016	–	1.225	–	1.016	–
H^+(5,6-diMeU)	1.320	0.979	1.023	111.8	1.319	0.979	1.021	113.7
Li^+(5,6-diMeU)	1.268	1.740	1.019	175.7	1.265	1.746	1.018	173.0
Na^+(5,6-diMeU)	1.259	2.100	1.017	176.7	1.257	2.105	1.018	172.7
K^+(5,6-diMeU)	1.253	2.471	1.017	176.1	1.250	2.480	1.017	172.8

[a] Rodgers and Armentrout [23].

est for substitution along the direction of the dipole moment, i.e., at the 3- and 6- positions. The effects of dimethylation are roughly additive such that the change in the dipole moments for 1,3-diMeU and 5,6-diMeU are nearly equal to the sum of the differences observed for the two corresponding methyluracils.

3.5. Alkali metal ion binding

In previous work [23] the preferred binding site for the alkali metal ions to U was found to be at the O4 position. The C=O–M^+ bond angle is very nearly linear but shifted slightly away from the adjacent NH group and the direction of the permanent dipole moment, Fig. 1. Changes in the structure of the nucleobase upon alkali metal ion complexation are minor (Table 5). An alternative binding site at the O2 position is found to be slightly less favorable by 14.4 kJ/mol for Li^+, 11.7 kJ/mol for Na^+, and 11.6 kJ/mol for K^+. In contrast, complexation of Li^+ to the π electrons of U was found to be 138 kJ/mol less favorable than binding at the O4 position [23]. Because methyl substituents are electron donating, methylation of uracil should slightly increase the π electron density of the aromatic ring making the π-complexes slightly more stable. However, this effect is expected to be very small. Therefore, calculations for other π-complexes were not pursued in the present work. The results for binding of alkali metal ions to the *x*MeU nucleobases are very similar to that found for U. The methyl groups are oriented to minimize steric repulsion within the molecule or complex. Based upon the ground state geometries found for the neutral and M^+(*x*MeU) complexes, it is clear that the repulsive interactions of the methyl group H atoms are greatest for interaction with M^+–O=C groups,

Table 6
Calculated enthalpies of deprotonation of methylated uracils at 0 K in kJ/mol[a]

Species	Deprotonation site	Theory (MP2(full))			CBS-Q	Literature	
		D_e	D_0[b]	$D_{0,BSSE}$[c]		Experiment[d]	B3LYP[d]
U	N1	1422.5	1387.0	1377.0	1390.7	1393 (17)[e]	1391[f]
							1377[g]
3-MeU	N1	1431.2	1395.0	1384.9		1393 (8)[g]	1386[g]
5-MeU	N1	1429.6	1393.8	1383.8			
6-MeU	N1	1428.1	1392.2	1382.1		1385 (2)[g]	1383[g]
5,6-diMeU	N1	1433.2	1397.4	1387.3		1393 (8)[g]	1388[g]
U	N3	1475.3	1436.5	1426.4	1440.2	1452 (17)[e]	1447[f]
							1433[g]
1-MeU	N3	1479.5	1441.1	1430.9		1456 (13)[g]	1438[g]
5-MeU	N3	1477.3	1438.7	1428.6			
6-MeU	N3	1480.8	1442.1	1432.1		1473 (21)[g]	1440[g]
5,6-diMeU	N3	1484.3	1445.3	1435.2		1460 (13)[g]	1442[g]

[a] MP2(full)/6–311+*G*(2d,2p)//MP2(full)/6–31*G**.
[b] Also includes ZPE corrections.
[c] Also includes BSSE corrections.
[d] Measured values from ion-molecule reaction bracketing, calculated values determined at the B3LYP/6–31+*G** level of theory.
[e] Kurinovich and Lee [64].
[f] Chandra et al. [63].
[g] Kurinovich and Lee [62].

less for N–H groups, still less for C=O groups, and least for adjacent C–H groups. Alkali metal ion binding to the *x*MeU nucleobases at the O4 position is again preferred over the O2 position. The absolute binding affinity is found to depend strongly upon the alkali metal ion and to a much lesser extent upon the position(s) of methyl substitution. In contrast, the relative stability of the O4 and O2 conformers is found to depend slightly upon the alkali metal ion and to a much greater extent upon the position(s) of methyl substitution. Methylation at the N1 position (1-MeU and 1,3-diMeU) enhances the absolute binding affinity at O4 to a much greater extent than for binding at O2, resulting in the largest differences in the stability of the O2 and O4 conformers, 18.6–22.9 kJ/mol. Methylation at the C5 position (5-MeU and 5,6-diMeU) enhances the binding affinity at O2 to a much greater extent than to O4, resulting in the smallest differences in stability of the O2 and O4 conformers, 4.8–9.5 kJ/mol. Methylation at the N3 and C6 (3-MeU and 6-MeU) positions enhances the binding affinities of the O2 and O4 positions by nearly equal amounts such that the difference in stability of the O2 and O4 conformers is similar to that of U, 12.9–16.8 kJ/mol.

3.6. Proton affinities

The preferred site of protonation to U is also at the O4 position, but results in greater structural perturbations than alkali metalation. The C=O–H^+ bond angle is 112.4° with the proton again directed away from the adjacent NH group. This indicates sp^2 hybridization, in contrast to the C=O–M^+ bond angles which are nearly linear. Three alternate and less stable proton binding sites are found with similar C=O–H^+ bond angles (Table 4). The second most favorable binding site

Table 7
Calculated hydrogen bond lengths and enthalpies of base pairing A::*x*MeU and Na^+(A::*x*MeU) at 0 K in kJ/mol[a]

Species	Hydrogen bond lengths (Å)		Enthalpies of base pairing (kJ/mol)		
	N···HN	NH···O	D_e	D_0[b]	$D_{0,BSSE}$[c]
A::U	1.830	1.929	69.9	63.9	51.0
Na^+N3(A::U)	1.831	1.927	88.0	82.1	68.4
Na^+N7/NH_2(A::U)	1.950	1.815	86.6	81.2	68.0
Na^+O2(A::U)	1.894	2.240	124.9	117.5	99.9
Na^+O4(A::U)	1.986	–	114.4	105.8	91.4
A::1-MeU	1.836	1.917	71.2	65.1	52.0
A::3-MeU	–	1.953	37.6	31.5	23.5
A::5-MeU	1.834	1.929	69.9	63.7	50.6
A::6-MeU	1.835	1.920	70.5	64.6	51.6
A::1,3-diMeU	–	1.943	38.5	32.7	24.6
A::5,6-diMeU	1.835	1.925	69.8	63.6	51.0

[a] MP2(full)/6–311+*G*(2d,2p)//B3LYP/6–31*G**.
[b] Also includes ZPE corrections.
[c] Also includes BSSE corrections.

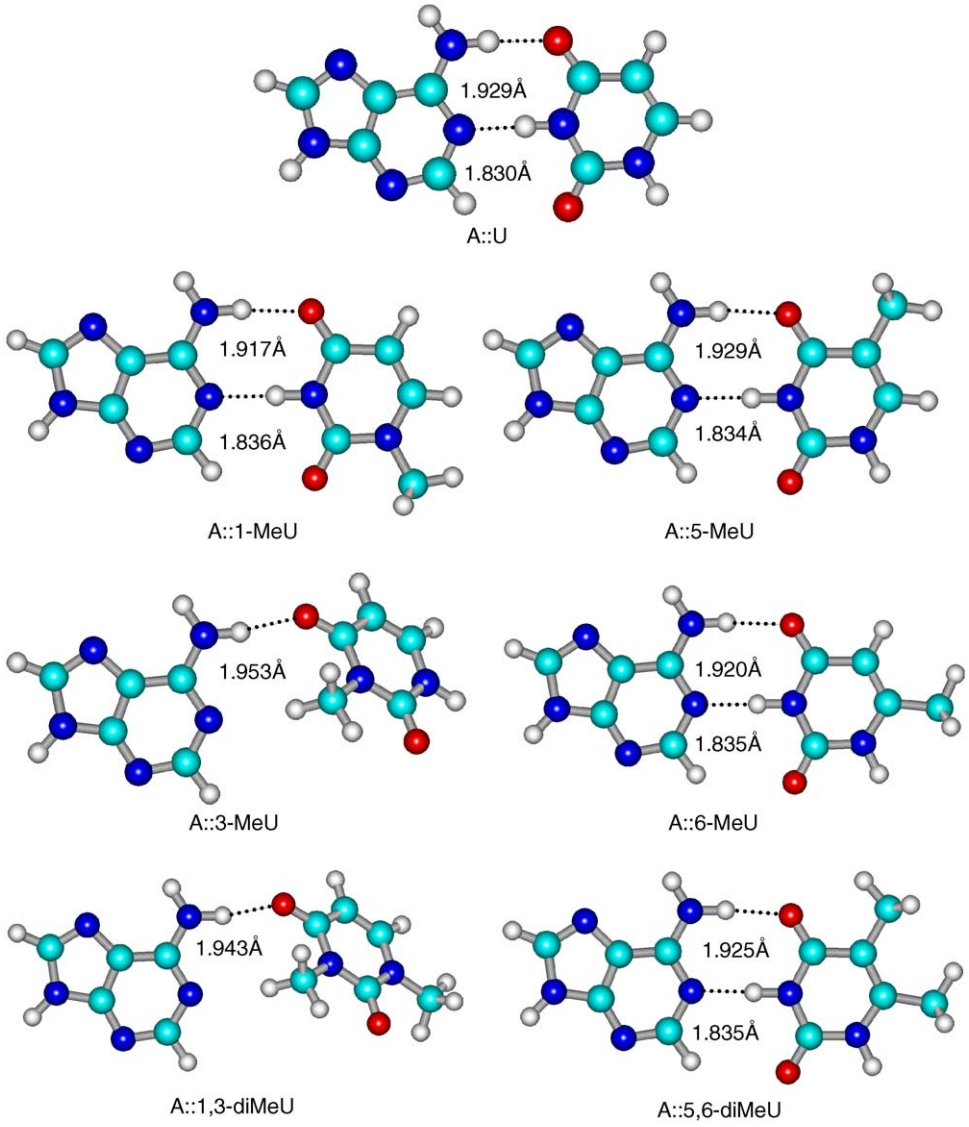

Fig. 5. MP2(full)/6–31*G** optimized geometries of A::*x*MeU base pairs, where *x*MeU = U, 1-MeU, 3-MeU, 5-MeU, 6-MeU, 1,3-diMeU, and 5,6-diMeU.

is also at the O4 position with the proton directed toward the adjacent NH group. Proton binding at this site is less favorable by 9.7 kJ/mol. The other two favorable binding sites are at the O2 position with the proton directed toward N1H being more favorable than toward N3H. Proton binding at these sites is less favorable than in the ground state O4 binding conformation by 29.9 and 34.7 kJ/mol, respectively. The results for proton binding to the *x*MeU nucleobases are very similar to those found for U. In all cases, methylation increases the proton affinity of all four binding sites, by 8.5–40.6 kJ/mol depending upon the position(s) and extent of methylation. The O4 sites are stabilized to a greater extent than the O2 sites in 1-MeU, 6-MeU and 1,3-diMeU, resulting in the largest differences between the proton affinities (PAs) of the O2 and O4 sites. Both sites are stabilized by an approximately equal extent in 3-MeU and 5,6-diMe. In contrast, proton binding at O2 is stabilized to a greater extent than the O4 site in 5-MeU, resulting in the smallest differences in the PAs of the O2 and O4 sites of all of the *x*MeU nucleobases. These differences in the stabilization of the O2 and O4 sites result in different relative PA orderings for binding at these sites.

3.7. Acidities

The gas phase acidities of uracil and its methylated analogs calculated at the MP2(full)/6–311+*G*(2d,2p)//MP2(full)/6–31*G** and CBS-Q levels of theory are summarized in Table 6. The N1 position of uracil is found to be considerably more acidic than the N3 position, by 49.4 kJ/mol. The CBS-Q calculations suggest that MP2 overestimates the N1 and N3 acidities of U, but finds that the relative acidities are accurately reproduced. Thus, the trends in the MP2 acidities should be a good descriptor of the influence of methylation on the acidity of the N1 and N3 sites. Methyl substi-

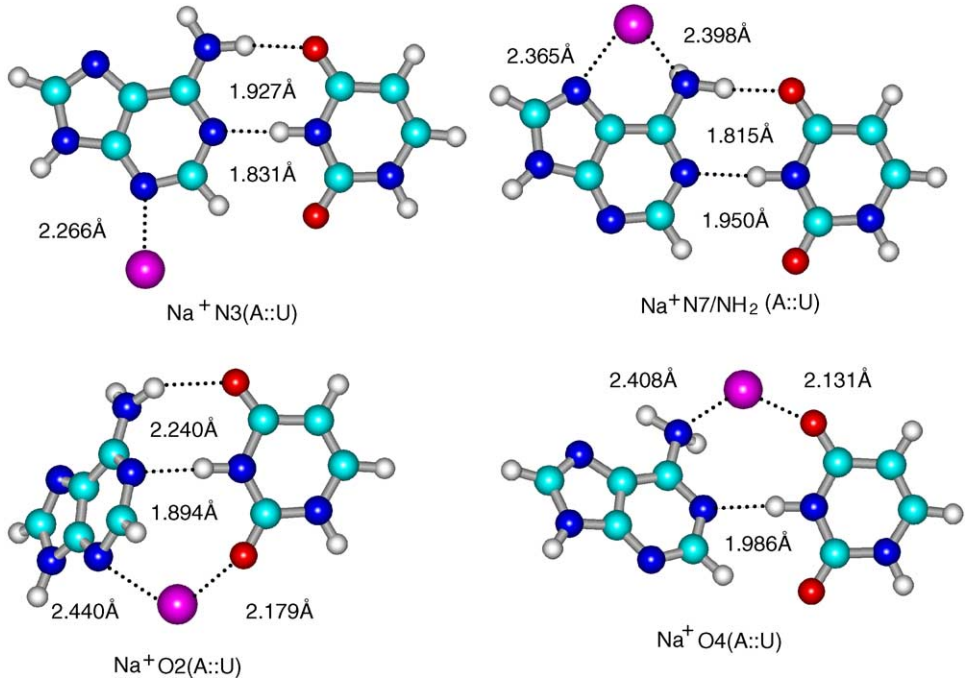

Fig. 6. MP2(full)/6–31*G** optimized geometries of Na^+X (A::U) base pairs, where *X* = N3, N7/NH_2, O2, and O4.

tution leads to a small decrease in the acidity of both sites, by 7.9, 6.8, and 5.1 kJ/mol at the N1 position for 3-MeU, 5-MeU, and 6-MeU, and by 4.5, 2.2, and 5.7 kJ/mol at the N3 position for 1-MeU, 5-MeU, and 6-MeU, respectively. Dimethylation, 5,6-diMeU, decreases the acidity, even further, by 10.3 kJ/mol for N1 and 8.8 kJ/mol for N3 as compared to uracil.

3.8. Effects of methylation on base pairing

In nucleic acids, uracil and thymine base pair with adenine via two hydrogen bonds in which the O4 and N3H atoms of U (T = 5-MeU) interact with one of the amino H atoms and N1 of adenine (A), respectively. In the calculations performed here, we only consider such Watson–Crick base pairing. The geometry optimized structures of the A::U and A::*x*MeU Watson–Crick base pairs are shown in Fig. 5. The base pairing energy of the A::U base pair is calculated to be 51.0 kJ/mol. In general, methylation is found to have very little impact on the hydrogen bonding interactions in these base pairs except for when methylation occurs at the N3 position. Methylation at N1 and N6 increases the pairing energy by 1.0 and 0.6 kJ/mol, respectively, whereas methylation at C5 decreases the pairing energy by 0.4 kJ/mol. The effects of dimethylation at the C5 and C6 positions appear to cancel and do not alter the base pairing energy as compared to the A::U base pair. In contrast, methylation at the N3 position obviously disrupts the normal hydrogen bonding interactions such that only one hydrogen bond is possible for the A::3MeU and A::1,3-diMeU base pairs. In all other cases, the base pairs are planar, but steric repulsion with the N3 methyl group causes the base to rotate out of the plane such that the dihedral angle between the planes of A and 3-MeU or 1,3-diMeU is nearly 25°. This leads to base pairing interactions that are weaker than in the A::U base pair by 27.5 and 26.4 kJ/mol, respectively.

3.9. Effects of alkali metalation on base pairing

Alkali metal ion binding to the A::U base pair was also examined. Four Na^+ binding sites were considered, binding at N3 or N7/NH_2 to A and O2 or O4 binding to U. The N1 site of A was not considered as this is expected to be much less favorable because both hydrogen bonding interactions in the base pair would be disrupted by metal ion binding at this site. In addition, binding at this site would also result in significant distortion of the alignment of the bases, and would cause puckering of the nucleotide backbone. Such puckering would lead to further losses in stability associated with disruption of the hydrogen bonding interactions in neighboring base pairs. Other alternative Na^+(A::U) structures were not considered because the backbone of the nucleotide would not allow the bases to freely rotate to maximize the binding interaction with the sodium ion.

Alkali metal ion binding is found to increase the stability of the A::U base pair regardless of the binding site. Binding to A at N3 or the N7/NH2 chelation site increases the base pairing energy by 17.4 and 17.0 kJ/mol, respectively. This increase in the stability of the base pair arises from the increased acidity of the amino hydrogen atom upon Na^+ binding. This is clearly seen as a shortening of the NH···O hydrogen bond length. The effect is smaller in the Na^+N3(A::U) base pair than the Na^+N7/NH_2(A::U) base pair where the amino group is directly involved in the binding. Overall, the

increase in stability is very similar for both of these base pairs because a lengthening of the N···HN hydrogen bond in the Na^+N7/NH_2(A::U) accompanies the shortening of the NH···O hydrogen bond length. Binding to U at O2 or O4 increases the pairing energy to an even greater extent, by 48.9 and 40.4 kJ/mol, respectively. At first glance this is somewhat surprising because the NH···O hydrogen bond is disrupted by the binding of the Na^+ ion in both of these base pairs. The enhancement in the pairing energy arises partly from the effects of metal ion binding on the acidity of the N3H and basicity of the O4 positions, but is mainly derived from additional metal chelation interactions with the second nucleobase.

The Na^+N3(A::U) base pair is the only metalated base pair that remains planar. The Na^+N7(A::U) base pair distorts slightly from planarity to allow Na^+ to bind at the $N7/NH_2$ chelation site without loss of the hydrogen bonding interaction between the amino group and the O4 position of uracil. The Na^+O2(A::U) base pair also deviates from planarity to allow Na^+ to simultaneously interact with the O2 site in U and the N3 site in A. Both hydrogen bonds are maintained, but are obviously somewhat compromised by the nonplanar arrangement of the two bases. The Na^+O4(A::U) base pair deviates from planarity to allow Na^+ to simultaneously interact with the O4 site in U and to chelate with the amino group of A. Optimization of this chelation interaction disrupts the hydrogen bond between O4 and the amino hydrogen atom. The enhancements in the metal ion binding interactions clearly overcome the loss of stability associated with the non-ideal hydrogen bonding geometries in these complexes.

4. Discussion

4.1. Comparison between theory and experiment

The measured alkali metal ion affinities of U and the methylated uracils measured by guided ion beam mass spectrometry and calculated here are summarized in Table 4. The agreement between theory and experiment is illustrated in Fig. 7. It can be seen that agreement is reasonable over the nearly 150 kJ/mol variation in the binding affinities measured here. For the 15 systems examined here, the mean absolute deviation (MAD) between theory and experiment is 10.6 ± 10.2 kJ/mol. This MAD is slightly greater than the estimated computational accuracy (~8 kJ/mol as determined for complexes to Na^+ [58]) and approximately twice as large as the average experimental error, 5.1 ± 1.6 kJ/mol. Careful inspection of the data makes it clear than the principal contributors to the deviations are the Li^+ systems. For the Li^+ complexes, the MAD is 23.9 ± 5.0 kJ/mol, while the Na^+ and K^+ systems have a MAD of 3.9 ± 2.2 kJ/mol. The results are very similar in all respects when U and 5-MeU are also included in the comparison, but the MADs decrease by 0.2 to 2.4 kJ/mol. The large disparity between theory and experiment for the Li^+ complexes suggests that either theory underestimates or experiment overestimates the BDEs to Li^+. A possible reason

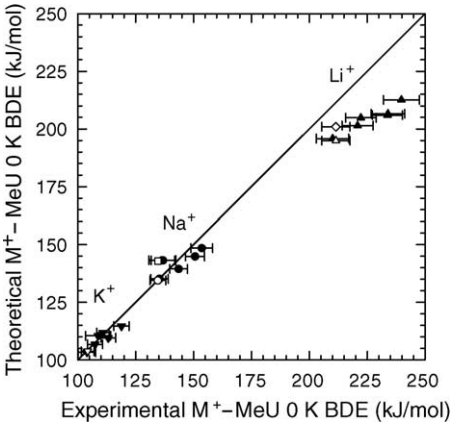

Fig. 7. Theoretical versus experimental 0 K bond dissociation energies of M^+–*x*MeU (in kJ/mol), where $M^+ = Li^+$ (▲,△,◊), Na^+(●,○,□), and K^+(▼,▽) and *x*MeU = U, 1-MeU, 3-MeU, 1,3-diMeU, 5-MeU, 6-MeU, and 5,6-diMeU. All theoretical values are from MP2(full)/6–311+*G*(2d,2p) calculations except for the Li^+(*x*MeU) complexes where CBS-Q values are shown (◊,□), Values for uracil are shown as open symbols [23].

for the measured BDEs to Li^+ being too large would arise if low mass discrimination in the quadrupole mass filter made if difficult to detect Li^+ near threshold. This possibility was eliminated in the present work using our new 1.7 MHz oscillator, which does not suffer from the low mass discrimination observed with our alternative 880 kHz oscillator as discussed in the Section 2. Thus, the disparity between theory and experiment for the Li^+ systems is not the result of instrumental artifacts. This disparity may be the result of the higher degree of covalency in the Li^+-nucleobase interaction. The additional covalency of the metal-nucleobase interaction in the Li^+ systems compared to those for Na^+ and K^+ suggests that this level of theory may be inadequate for a complete description of the former systems. To examine this possibility further, we compare to BDEs using the complete basis set extrapolation protocol, CBS-Q, which in principle should lead to more accurate binding energies. Unfortunately, these calculations were beyond the computational resources available to us for all of the M^+(*x*MeU) complexes, but were possible for the M^+(U) complexes. The Li^+–U BDE increases by 6.0 kJ/mol from MP2 to CBS-Q, bringing the measured value into much better agreement with theory. However, the reliability of this calculation is brought into question when the Na^+–U and K^+–U BDEs are examined. The Na^+–U BDE increases by 8.4 kJ/mol from MP2 to CBS-Q resulting in poorer agreement with the measured value. The comparison for K^+–U is even worse. The CBS-Q method predicts that the K^+(U) complex is less stable than the isolated alkali metal ion and nucleobase, (i.e., K^+(U) is not bound). This is clearly not the case, or we would not observe the formation of this complex under our experimental conditions. Therefore, the CBS-Q protocol is clearly unreliable for determining the BDEs in the M^+(U) systems. Similar results with regard to the reliability of the CBS-Q protocol have previously been documented [56]. Thus, the level of theory required for an accurate de-

scription of the binding in the Li^+(*x*MeU) complexes is still unresolved. Because such disparities have been observed for other Li^+(ligand) complexes previously investigated, we are currently investigating this issue in another study for a whole host of Li^+(ligand) complexes [59]. Although we have not completely resolved this issue yet, preliminary results suggest that strongly binding ligands (i.e., those with large dipole moments or polarizabilities) are able to penetrate the core of the Li^+ as a result of its small size. Therefore, accurate theoretical BDEs for Li^+(ligand) complexes can only be obtained by using basis sets that allow more effective core penetration than the 6–31*G** and 6–311+*G*(2d,2p) basis sets or the CBS-Q protocol allow.

4.2. Conversion from 0 to 298 K

To allow comparison to previous literature values and standard experimental conditions, we convert the 0 K BDEs determined here to 298 K BDEs and free energies. The enthalpy and entropy conversions are calculated using standard formulas and the vibrational frequencies and rotational constants determined for the MP2(full)/6–31*G** optimized geometries, which are given in Tables 1 and 2. Table 8 lists the 0 and 298 K enthalpy, free energy, and enthalpic and entropic corrections for all of the M^+(*x*MeU) systems.

4.3. Trends in the binding of alkali metal ions to the methylated uracils

In all of the M^+(*x*MeU) systems, the measured BDE varies with the alkali metal ion such that Li^+ binds ∼60% more strongly than Na^+, which in turn binds ∼30% more strongly than K^+. This trend confirms that the binding in these complexes is largely electrostatic. The smaller alkali metal ions bind more strongly because the alkali metal ion-nucleobase bond distance is shorter resulting in stronger ion-dipole and ion-induced dipole interactions.

Theoretical examination of the charge retained on the alkali metal ion in these M^+(*x*MeU) complexes shows that Li^+ retains less charge (0.70–0.74 e) than Na^+ (0.96–0.98 e), which retains less charge than K^+ (0.98–0.99 e). This trend again confirms the electrostatic nature of the bonding, but also demonstrates that there is a moderate degree of covalent character in the metal-nucleobase interaction for the Li^+(*x*MeU) complexes as discussed above. The shorter Li^+–O bond distance allows Li^+ to more effectively withdraw electron density from the neutral nucleobase, thus, reducing the charge retained on the alkali metal ion.

4.4. Influence of methylation on the alkali metal ion binding affinities of uracil

As discussed above, the variation in the M^+–*x*MeU BDEs with M^+ indicates that the binding in these complexes is largely electrostatic. Therefore, the strength of the binding in these complexes should be controlled by ion-dipole and ion-induced dipole interactions. The effect that the methyl substituent(s) have upon the binding can be examined by comparing these systems to the unsubstituted uracil molecule. The polarizability of uracil is estimated to be 8.69 $Å^3$ and increases to 11.48 $Å^3$ upon methylation and to 13.30 $Å^3$ upon dimethylation [25]. The polarizability is

Table 8
Enthalpies and free energies of metal ion binding to methylated uracils at 298 K in kJ/mol[a]

System	ΔH_0	ΔH_0[b]	ΔH_{298}-ΔH_0[b]	ΔH_{298}	ΔH_{298}[b]	$T\Delta S_{298}$[b]	ΔG_{298}	ΔG_{298}[b]
Li^+(U)[c]	211.5 (6.1)	194.9	2.3 (0.2)	213.8 (6.1)	197.2	27.6 (0.4)	186.2 (6.1)	169.6
Na^+(U)[c]	134.6 (3.4)	135.5	1.1 (0.1)	135.7 (3.4)	136.6	27.4 (0.5)	108.3 (3.7)	109.2
K^+(U)[c]	104.3 (2.8)	103.8	0.7 (0.1)	105.0 (2.8)	104.5	26.8 (0.6)	78.2 (2.9)	77.7
Li^+(1-MeU)	234.0 (7.2)	206.6	2.4 (0.2)	236.4 (7.2)	209.0	28.6 (0.4)	207.8 (7.2)	180.4
Na^+(1-MeU)	150.7 (4.1)	144.9	1.2 (0.2)	151.9 (4.1)	146.1	28.3 (0.5)	123.6 (4.1)	117.8
K^+(1-MeU)	110.9 (2.7)	111.9	0.7 (0.1)	111.6 (2.7)	112.6	27.6 (0.6)	84.0 (2.8)	85.0
Li^+(3-MeU)	220.9 (6.7)	201.4	2.5 (0.2)	223.4 (6.7)	203.9	28.3 (0.4)	195.1 (6.7)	175.6
Na^+(3-MeU)	143.6 (3.8)	139.5	1.2 (0.2)	144.8 (3.8)	140.7	28.1 (0.5)	116.7 (3.8)	112.6
K^+(3-MeU)	107.5 (3.3)	106.8	0.8 (0.1)	108.3 (3.3)	107.6	27.3 (0.5)	81.0 (3.3)	80.3
Li^+(5-MeU)[c]	210.1 (7.0)	195.8	2.3 (0.2)	212.4 (7.0)	198.1	27.6 (0.4)	184.8 (7.0)	170.5
Na^+(5-MeU)[c]	135.3 (3.8)	135.2	1.1 (0.1)	136.4 (3.8)	136.3	27.6 (0.5)	108.8 (3.8)	108.7
K^+(5-MeU)[c]	104.0 (3.8)	103.4	0.6 (0.1)	104.6 (3.8)	104.0	26.8 (0.6)	77.8 (3.8)	77.2
Li^+(6-MeU)	222.3 (6.6)	204.8	2.2 (0.2)	224.5 (6.6)	207.0	27.3 (0.4)	197.2 (6.6)	179.7
Na^+(6-MeU)	136.6 (5.8)	143.3	1.0 (0.1)	137.6 (5.8)	144.3	27.3 (0.5)	110.3 (5.8)	117.0
K^+(6-MeU)	108.8 (5.4)	110.5	0.6 (0.1)	109.4 (5.4)	111.1	26.8 (0.6)	82.6 (5.4)	84.3
Li^+(1,3-diMeU)	239.8 (6.6)	212.6	2.5 (0.2)	242.3 (6.6)	251.1	29.0 (0.4)	213.3 (6.6)	186.1
Na^+(1,3-diMeU)	153.6 (4.7)	148.5	1.3 (0.2)	154.9 (4.7)	149.8	28.8 (0.5)	126.1 (4.7)	121.0
K^+(1,3-diMeU)	118.9 (3.3)	114.7	0.8 (0.1)	119.7 (3.3)	115.5	27.9 (0.5)	91.8 (3.3)	87.6
Li^+(5,6-diMeU)	233.8 (6.5)	206.0	2.4 (0.2)	236.2 (6.5)	208.4	28.2 (0.4)	208.0 (6.5)	180.2
Na^+(5,6-diMeU)	136.8 (5.1)	143.2	1.1 (0.1)	137.9 (5.1)	144.3	26.3 (0.5)	111.6 (5.1)	118.0
K^+(5,6-diMeU)	113.2 (3.2)	109.6	0.6 (0.1)	113.8 (3.2)	110.2	26.6 (0.6)	87.2 (3.3)	83.6

[a] Uncertainties are listed in parentheses.
[b] Ab initio values from calculations at the MP2(full)/6–311+*G*(2d,2p)//MP2(full)/6–31*G** level of theory with frequencies scaled by 0.9646.
[c] Rodgers and Armentrout [23].

not expected to vary significantly with the position(s) of the methyl substituent(s), and the additivity method we used to estimate these polarizabilities is not sensitive to such structural differences. Therefore, the ion-induced dipole attractions should roughly correlate with the extent of methylation. This suggests that if the ion-induced dipole interactions dominate the binding, the M^+–*x*MeU BDEs should follow the order: 1,3-diMeU ≈ 5,6-diMeU > 1-MeU ≈ 3-MeU ≈ 5-MeU ≈ 6–MeU > U. Indeed, the binding affinity of U is observed to increase upon methyl substitution in all cases except for the 5-MeU complexes, where the interactions are essentially unaffected, Table 4. Similarly, the increase in the M^+–*x*MeU BDE is generally larger for the dimethyluracils than the methyluracils. However, ion-dipole interactions should also be important in determining the strength of binding in these complexes. The ion-dipole attractions should correlate with the dipole moments of these nucleobases. This suggest that if the ion-dipole interactions dominate the binding, the M^+–*x*MeU BDEs should follow the order: 6-MeU ≈ 5,6-diMeU > 1-MeU > U ≈ 5-MeU ≈ 1,3-diMeU > 3-MeU. Examination of the experimental and theoretical data shows that neither of these relative binding orders are entirely preserved. In fact, no systematic relative ordering in the M^+–*x*MeU BDEs is preserved for all of the alkali metal ions. However, the relative ordering most consistent with the experimental data is: 1,3-diMeU > 1–MeU > 5,6-diMeU > 6-MeU > 3-MeU > 5-MeU ≈ U. The observed trend does not correlate directly with either the polarizabilities or dipole moments of these *x*MeU nucleobases and indicates that *N*-methylation leads to a greater increase in the binding interaction than does *C*-methylation. The trend in the BDEs can be reconciled however, when a balance of all three of these factors are considered.

4.5. Influence of methylation on the proton affinity of uracil

The proton affinities of uracil and its methylated analogs calculated at the MP2(full)/6–311+*G*(2d,2p)//MP2(full)/6–31*G** and CBS-Q levels of theory are summarized in Table 4. Also given in Table 4, are literature values for the proton affinities of U and 5-MeU measured by ion molecule reaction bracketing studies [60,61]. The relative theoretical PAs of the *x*MeU nucleobases follow the order: 1,3-dimeU > 5,6-diMeU > 1-MeU > 3-MeU > 6-MeU > 5-MeU > U for binding at O4. A different relative ordering is found for binding at O2: 1,3-dimeU > 5,6-diMeU > 3-MeU > 5-MeU > 1-MeU > 6-MeU > U. These trends parallel that expected based upon the polarizabilities of these ligands for proton binding at either site. As found for the binding of alkali metal ions to these nucleobases, *N*-methylation results in a greater increase in the O4 proton affinity than observed for *C*-methylation.

4.6. Influence of methylation on the acidity of uracil

The gas phase acidities of uracil and its methylated analogs calculated at the MP2(full)/6–311+*G*(2d,2p)//MP2(full)/6–31*G** and CBS-Q levels of theory are summarized in Table 6. Also given in Table 6 are literature values for these acidities calculated at the B3LYP/6–31+*G** [62] and B3LYP/6–31++*G*** levels of theory [63] and values measured by ion molecule reaction bracketing studies [62,64]. The MP2 values calculated here for the acidity of the N1 position are all within 1 kJ/mol of those calculated at the B3LYP/6–31+*G** level of theory. In contrast, our calculations find that the N3 position is more acidic by 7–8 kJ/mol than determined at the B3LYP/6–31+*G** level of theory. Calculations at the B3LYP/6–31++*G*** level of theory suggests that the N1 and N3 positions of U are 14 kJ/mol less acidic than found at the B3LYP/6–31+*G** level of theory. No calculations at the B3LYP/6–31++*G*** level of theory were carried out for the *x*MeU nucleobases. The use of a much larger basis set should lead to more accurate results, suggesting that the MP2 and B3LYP calculations with the smaller basis set for the other *x*MeU nucleobases are also overestimated. Indeed, the B3LYP/6–31++*G*** calculations are in better agreement with the experimental values determined from ion-molecule reaction bracketing studies. The CBS-Q calculations also confirm that the N1 and N3 sites are less acidic. However, the CBS-Q calculations suggest that the N1 site is less acid by 14 kJ/mol, whereas the N3 site is less acidic by only 7 kJ/mol. The trends in the calculated values combined with the decrease in acidity expected based on the CBS-Q results suggest that the N1 site of the *x*MeU nucleobases should be 2–11 kJ/mol less acidic than measured in the ion-molecule reaction bracketing studies, whereas the N3 site should be less acidic by 4–27 kJ/mol. However, it should be noted that the experimental and theoretical trends are consistent within the measured experimental errors.

4.7. Implications for nucleic acid stability

The present results allow predictions for metal-induced and methylation-induced stability changes in nucleic acids. The preferred alkali metal ion binding sites to isolated A and U are the N7/NH2 chelation site and O4, respectively. However, we previously noted that binding of alkali metal ions to either of these sites might tend to disrupt hydrogen bonding interactions in A:U (A:T) base pairs [23]. Disruption of a single hydrogen bond in an A::U base pair costs about 27 kJ/mol, more than the calculated difference in binding affinities of the N3 and N7/NH2 sites in A or the O2 and O4 sites in U. Thus, alkali metal ions may preferentially bind at the N3 or O2 sites of the A::U base pair, such that hydrogen bonding between the bases is not disrupted. The structures and relative stability of the Na^+(A::U) complexes indicate that binding to U is preferred over A. Binding at O4 with the alkali metal ion chelating to the amino group is found to be the most favorable even though this disrupts one of the hydrogen bonds. Binding to U at O2 and with the alkali metal ion chelating to N3 is only 1.1 kJ/mol less favorable, while binding to A at the N7/NH_2 and N3 sites are 28.3 and 45.5 kJ/mol less favorable than binding at O4. Binding

of an alkali metal ion is also found to increase the pairing energy by 17.0 to 48.9 kJ/mol and, thus, is expected to increase the stability of the nucleic acid. However, the most favorable binding modes of the alkali metal ion to the A::U base pair require that it distort from planarity. Such distortions may weaken hydrogen-bonding interactions between nearby base pairs. This would reduce the stabilization gained from the additional chelation interactions with the alkali metal ion and impact the stability of the nucleic acid to a lesser extent than for the isolated base pair. The presence of the alkali metal ion would also tend to increase the strength of base stacking interactions via cation-π interaction of the alkali metal ion with the adjacent nucleobases. Thus, alkali metal ion binding to the bases should increase the stability of nucleic acids by reducing the charge on the nucleic acid via a zwitterion effect as well as through additional noncovalent interactions between the alkali metal ion and the nucleobases.

Methylation at any site except N3 is expected to influence the stability of nucleic acids to a much lesser extent than alkali metal ion binding. Methylation at N1, C5, or C6 has very little impact on the strength of hydrogen bonding interactions between A and U (<1 kJ/mol). In contrast, methylation at N3 decreases the stability of the A::U base pair by ~27 kJ/mol. Methylation at any site increases the polarizability of the nucleobase and would therefore tend to slightly increase the strength of stacking interactions between adjacent base pairs. Thus, a small increase in the stability of nucleic acids is expected upon methylation at any site except N3. Methylation at N3 disrupts one of the hydrogen-bonding interactions in the A::U base pair and causes a distortion from planarity. As for the alkali metal ions, such distortions might weaken hydrogen-bonding interactions between nearby base pairs, further reducing the stability of the nucleic acid.

5. Conclusions

The kinetic energy-dependence of the CID of $M^+(x\text{MeU})$, where $M^+ = Li^+$, Na^+, K^+, and xMeU = 1-MeU, 3-MeU, 6-MeU, 1,3-diMeU, and 5,6-diMeU, with Xe is examined in a guided ion beam mass spectrometer. The dominant dissociation process is loss of the intact neutral nucleobase. Thresholds for these processes are determined after consideration of the effects of reactant internal energy, multiple collisions with Xe, and lifetime effects. Insight into the structures and binding of alkali metal ions to the xMeU nucleobases as well as the effects of methylation on the proton affinities, acidities, and base pairing energies is provided by ab initio calculations performed at the MP2(full)/6–311+G(2d,2p)//MP2(full)/6–31G* level of theory. Reasonable agreement between the experimentally determined and theoretically calculated M^+-xMeU BDEs is obtained, although the calculated values are systematically low for the Li^+ complexes. The excellent agreement between theory and experiment for the $Na^+(x\text{MeU})$ and $K^+(x\text{MeU})$ complexes suggest that these systems can act as reliable thermochemical anchors for other studies. In addition, parallel studies of a variety of Li^+(ligand) complexes suggest that the level of theory employed in the present work does not adequately describe the Li^+-ligand interaction such that we believe that the experimental Li^+-xMeU BDEs are more reliable than the corresponding calculated values. Further, the combined experimental and theoretical results provide an understanding of the effects of alkali metal ion binding and methylation on the structure and stability of nucleic acids. The present results suggest that alkali metal ion binding should tend to increase the stability of nucleic acids by reducing the charge on the nucleic acid in a zwitterion effect as well as through additional noncovalent interactions between the alkali metal ion and the nucleobases. In contrast, methylation is expected to almost negligibly impact the stability except when methylation occurs at N3 where a significant destabilization of the nucleic acid is anticipated.

Acknowledgement

This work is supported by the National Science Foundation, Grant CHE-0138504. In honor of W.L. Hase on the occasion of his 60th birthday, a great friend, colleague, and theoretician. In special thanks for his many contributions to the development of chemical reaction dynamics and our current understanding of statistical theories for unimolecular dissociation and the reactivity of gaseous ions, the contributions in particular that have most impacted my research.

References

[1] W. Saenger, in: C.R. Cantor (Ed.), Principles of Nucleic Acid Structure, Springer-Verlag, Boston, 1984.
[2] G.L. Eichhorn, Adv. Inorg. Biochem. 3 (1981) 1.
[3] Y.A. Shin, G.L. Eichhorn, Biopolymers 16 (1977) 225.
[4] A.L. Lehninger, Biochemistry, The Molecular Basis of Cell Structure and Function, second ed., Worth Publishers, Inc., New York, 1977.
[5] F. Valeriote, G. Santelli, Pharmocol. Ther. 24 (1984) 107.
[6] C. Wasternack, B. Hause, Pharmazie 42 (1987) 73.
[7] R.C. Bohinski, Modern Concepts in Biochemistry, fifth ed., Allyn and Bacon, Inc., Massachusetts, 1987.
[8] P.C. Hanawalt, Mutation Research-DNA-Repair 485 (2001) 3.
[9] O. Dolgounitcheva, V.G. Zakrzewski, J.V. Oritiz, J. Phys. Chem. A 106 (2002) 8411.
[10] Q. Zhu, P.R. LeBreton, J. Am. Chem. Soc. 122 (2000) 12824.
[11] N.S. Kim, Q. Zhu, P.R. LeBreton, J. Am. Chem. Soc. 121 (1999) 11516.
[12] N.S. Kim, P.R. LeBreton, J. Am. Chem. Soc. 118 (1996) 3694.
[13] K.M. Youssef, E. Al-Abdullah, H. El-Khamees, Med. Chem. Res. 10 (2001) 404.
[14] P.W. Laird, R. Jaenisch, Ann. Rev. Gen. 30 (1996) 441.
[15] S. Takao, S. Akiyama, A. Nakajo, H. Yoh, M. Kitazono, S. Natsugoe, K. Miyadera, M. Fukushima, Y. Yamada, T. Aikou, Cancer Res. 60 (2000) 5345.
[16] C. Cole, D.S. Marks, M. Jaffa, I.J. Stratford, K.T. Douglas, S. Freeman, Anti-Cancer Drug Des. 14 (1999) 411.
[17] S. Matsushita, T. Nitanda, T. Furukawa, T. Sumizawa, A. Tani, K. Nishimoto, S. Akiba, K. Miyadera, M. Fukushima, Y. Yamada, H. Yoshida, T. Kanzaki, S. Akiyama, Cancer Res. 59 (1999) 1911.

[18] M. Grote, S. Noll, B. Noll, B. Johannsen, W. Kraus, Can. J. Chem. 82 (2004) 513.
[19] D.R. Imam, A.A. El-Barbary, C. Nielsen, E.B. Pedersen, Monatsh. Chem. 133 (2002) 723.
[20] I.I. Volchenskova, N.N. Maidanevich, L.I. Budarin, Inorg. Chim. Acta 79 (1983) 246.
[21] J. Baranowska-Kortylewicz, E.J. Pavlik, W.T. Smith, R.C. Flanigan, J.R. van Nagell, D. Ross, D.E. Kenady, Inorg. Chim. Acta 108 (1985) 91.
[22] Z. Yang, M.T. Rodgers, J. Am. Chem. Soc. 126 (2004) 16217.
[23] M.T. Rodgers, P.B. Armentrout, J. Am. Chem. Soc. 122 (2000) 8548.
[24] B.A. Cerda, C. Wesdemiotis, J. Am. Chem. Soc. 118 (1996) 11884.
[25] K. Miller, J. Am. Chem. Soc. 112 (1990) 8533.
[26] M.T. Rodgers, K.M. Ervin, P.B. Armentrout, J. Chem. Phys. 106 (1997) 4449.
[27] M.T. Rodgers, J. Phys. Chem. A 105 (2001) 2374.
[28] E. Teloy, D. Gerlich, Chem. Phys. 4 (1974) 417;
D. Gerlich, Diplomarbeit, University of Freiburg, Federal Republic of Germany, 1971;
D. Gerlich, In state-selected and state-to-state ion-molecule reaction dynamics. Part I. Experiment, in: C.-Y. Ng, M. Baer (Eds.), Advances in Chemical Physics Series, 82, Wiley, New York, 1992, p. 1.
[29] N.F. Dalleska, K. Honma, P.B. Armentrout, J. Am. Chem. Soc. 115 (1993) 12125.
[30] N. Aristov, P.B. Armentrout, J. Phys. Chem. 90 (1986) 5135.
[31] D.A. Hales, P.B. Armentrout, J. Cluster Sci. 1 (1990) 127.
[32] K.M. Ervin, P.B. Armentrout, J. Chem. Phys. 83 (1985) 166.
[33] N.F. Dalleska, K. Honma, L.S. Sunderlin, P.B. Armentrout, J. Am. Chem. Soc. 116 (1994) 3519.
[34] Gaussian 98, Revision A.11, Gaussian, Inc. Pittsburgh PA, 1998. M.J. Frisch, G.W. Trucks, H.B. Schlegel, G.E. Scuseria, M.A. Robb, J.R. Cheeseman, V.G. Zakrzewski, J.A. Montgomery Jr., R.E. Stratmann, J.C. Burant, S. Dapprich, J.M. Millam, A.D. Daniels, K.N. Kudin, M.C. Strain, O. Farkas, J, Tomasi, V. Barone, M. Cossi, R. Cammi, B. Mennucci, C. Pomelli, C. Adamo, S. Clifford, J. Ochterski, G.A. Petersson, P.Y. Ayala, Q. Cui, K. Morokuma, D.K. Malick, A.D. Rabuck, K. Raghavachari, J.B. Foresman, J. Cioslowski, J.V. Ortiz, B.B. Stefanov, G. Liu, A. Liashenko, P. Piskorz, I. Komaromi, R. Gomperts, R.L. Martin, D.J. Fox, T. Keith, M.A. Al-Laham, C.Y. Peng, A. Nanayakkara, C. Gonzalez, M. Challacombe, P.M.W. Gill, B. Johnson, W. Chen, M.W. Wong, J.L. Andres, C. Gonzales, M. Head-Gordon, E.S. Replogle, J.A. Pople.
[35] F. Muntean, P.B. Armentrout, J. Chem. Phys. 115 (2001) 1213.
[36] T.S. Beyer, D.F. Swinehart, Comm. Assoc. Compt. Machines 16 (1973) 379;
S.E. Stein, B.S. Rabinovitch, J. Chem. Phys. 58 (1973) 2438;
S.E. Stein, B.S. Rabinovitch, Chem. Phys. Lett. 49 (1977) 1883.
[37] J.A. Pople, H.B. Schlegel, K. Ragavachari, D.J. DeFrees, J.F. Binkley, M.J. Frisch, R.F. Whitesides, R.F. Hout, W.J. Hehre, Int. J. Quant. Chem. Symp. 15 (1981) 269;
D.J. DeFrees, A.D. McLean, J. Chem. Phys. 82 (1985) 333.
[38] F.A. Khan, D.E. Clemmer, R.H. Schultz, P.B. Armentrout, J. Phys. Chem. 97 (1993) 7978.
[39] W.J. Chesnavich, M.T. Bowers, J. Phys. Chem. 83 (1979) 900.
[40] See, for example, Figure 1 in N.F. Dalleska, K. Honma, P.B. Armentrout, J. Am. Chem. Soc. 115 (1993) 12125.
[41] P.B. Armentrout, J. Simons, J. Am. Chem. Soc. 114 (1992) 8627.
[42] M.T. Rodgers, P.B. Armentrout, Mass Spectrom. Rev. 19 (2000) 215.
[43] M.T. Rodgers, J. Phys. Chem. A 105 (2001) 8145.
[44] R. Amunugama, M.T. Rodgers, J. Phys. Chem. A 105 (2001) 9883.
[45] A.B. Valina, R. Amunugama, H. Huang, M.T. Rodgers, J. Phys. Chem. A 105 (2001) 11057.
[46] G. Vitale, A.B. Valina, H. Huang, R. Amunugama, M.T. Rodgers, J. Phys. Chem. A 105 (2001) 11351.
[47] H. Huang, M.T. Rodgers, J. Phys. Chem. A 106 (2002) 4277.
[48] R. Amunugama, M.T. Rodgers, J. Phys. Chem. A 106 (2002) 5529.
[49] R. Amunugama, M.T. Rodgers, J. Phys. Chem. A 106 (2002) 9092.
[50] R. Amunugama, M.T. Rodgers, J. Phys. Chem. A 106 (2002) 9718.
[51] Y. Chu, Z. Yang, M.T. Rodgers, J. Am. Soc. Mass Spectrom. 13 (2002) 453.
[52] M.T. Rodgers, P.B. Armentrout, J. Am. Chem. Soc. 124 (2002) 2678.
[53] R. Amunugama, M.T. Rodgers, Int. J. Mass Spectrom. 222 (2003) 431.
[54] R. Amunugama, M.T. Rodgers, Int. J. Mass Spectrom. 227 (2003) 1.
[55] R. Amunugama, M.T. Rodgers, Int. J. Mass Spectrom. 227 (2003) 339.
[56] N.S. Rannulu, R. Amunugama, Z. Yang, M.T. Rodgers, J. Phys. Chem. A 108 (2004) 6385.
[57] C. Ruan, M.T. Rodgers, J. Am. Chem. Soc. 126 (2004) 14600.
[58] P.B. Armentrout, M.T. Rodgers, J. Phys. Chem. A 104 (2000) 2238.
[59] M.T. Rodgers, P.B. Armentrout (in preparation).
[60] E.P. Hunter, S.G. Lias, Proton affinity evaluation, in: W.G. Mallard, P.J. Lindstrom (Eds.), NIST Chemistry WebBook, NIST Standard Reference Database Number 69, November, 1998. National Institute of Standards and Technology: Gaithersburg MD, 20899 (http://webbook.nist.gov).
[61] M.A. Kurinovich, L.M. Phillips, S. Sharma, J.K. Lee, Chem. Commun. (2002) 2354.
[62] M.A. Kurinovich, J.K. Lee, J. Am. Soc. Mass Spectrom. 13 (2002) 985.
[63] A.K. Chandra, M.T. Nguyen, T. Uchimaru, T. Zeegers-Juyskens, J. Phys. Chem. A 103 (1999) 8853.
[64] M.A. Kurinovich, J.K. Lee, J. Am. Chem. Soc. 122 (2000) 6258.